

7-5-2016

# Effect of the variable porosity on the heat transfer process in solar air receiver

Pei Wang

*Hohai University*, franciswp2012@163.com

D. Y. Liu

*Hohai University Changzhou*

Follow this and additional works at: [http://dc.engconfintl.org/porous\\_media\\_vi](http://dc.engconfintl.org/porous_media_vi)



Part of the [Engineering Commons](#)

---

## Recommended Citation

Pei Wang and D. Y. Liu, "Effect of the variable porosity on the heat transfer process in solar air receiver" in "Sixth International Conference on Porous Media and Its Applications in Science, Engineering and Industry", Eds, ECI Symposium Series, (2016). [http://dc.engconfintl.org/porous\\_media\\_vi/17](http://dc.engconfintl.org/porous_media_vi/17)

This Conference Proceeding is brought to you for free and open access by the Proceedings at ECI Digital Archives. It has been accepted for inclusion in Sixth International Conference on Porous Media and Its Applications in Science, Engineering and Industry by an authorized administrator of ECI Digital Archives. For more information, please contact [franco@bepress.com](mailto:franco@bepress.com).

## EFFECT OF THE VARIABLE POROSITY ON THE HEAT TRANSFER PROCESS IN SOLAR AIR RECEIVER

P. Wang

*Department of Renewable Energy Science and Engineering, Hohai University, Nanjing, China;*

### ABSTRACT

Solar air receiver is the core component of central receiver system (CRS) in solar thermal power plants due to the unique feature of some porous medium like silicon carbide foam ceramic and so on. In the air receiver, the porous material receives the concentrated sunlight from the heliostat field and heats up the pumped inlet air by convection and radiation. The incident radiation is distributed in the inner space of the porous medium rather than located on the boundary of the heated face in the front of the receiver. Aiming at this phenomenon which called volumetric effect, we propose a novel solar air receiver using the porous medium with variable porosity along the incident direction to optimize its heat transfer process and increase the thermal efficiency of the receiver. For this kind of porous medium, the effect of the variability of the porosity  $\phi$  on the temperature and radiative heat flux distributions and also the thermal efficiency of the air receiver will be analyzed systematically. Our analysis demonstrated that the structure with variable porosity will enhance the transfer of radiative energy into the porous medium, consequently decreases the thermal radiative loss at the inlet and increases the thermal efficiency of the air receiver.

### INTRODUCTION

Porous media is widely utilized in many modern industrial applications involving heat transfer processes such as solar thermal utilization, nuclear waste repository, heat pipes, combustion, heat transfer enhancement etc. One area of utilization is the receiver (Aacutevila AL 2011) of a central receiver system (CRS) in solar thermal power plants due to the unique feature of silicon carbide (SiC) foam ceramic, such as large specific area, high conductivity and thermal shock resistance. In CRS, the porous material receives the concentrated sunlight from the heliostat field and heats up the pumped inlet air by convection and radiation.

Investigate on variants in local thermal non-equilibrium model was given by (Alazmi B, Vafai K 2000) considering the effect of non-Darcy, dispersion, non-equilibrium and variable porosity. The effect of different boundary

conditions under LTNE conditions was given by (Yang K, Vafai K 2010). However for the high temperature over thousands, thermal radiation behavior can not be neglected. Its impact on conductive heat transfer in a packed bed has been analyzed by (Singh BP, Kaviany M 1991). Aim at the radiation transfer in the porous media in some typical industrial device, (Wang P, Vafai K, and Liu DY 2014) performed a numerical analysis focus on the LTNE model coupled with radiation transfer. The mechanism of the influence of the radiation transfer on the coupled heat transfer process with conduction and convection in the media was revealed; (Flamant G, Olalde G 1983) focus on the radiation heat transfer process in a double layers structure (glass bed and SiC porous layer) experimentally.

When considering the collimated incident radiation, the distribution of radiative energy changes in the incident direction should be taken into account simultaneously with convection processes. Hence, the purpose of this study is to understand the role of the collimated incident radiation on the convective heat transfer in air receiver under LTNE conditions. In this work, the temperature fields for the solid matrix and fluid phases will be analyzed while incorporating the local thermal non-equilibrium along with the differential approximation (P-1 model). The effect of intrinsic properties and optic parameters will be discussed respectively.

### NOMENCLATURE

$c_p$	Specific heat of fluid at constant pressure [J kg <sup>-1</sup> K <sup>-1</sup> ]
$d_p$	Pore diameter [m]
$E_b$	Blackbody emissive power
$F$	Inertial coefficient
$G$	Incident radiation
$h_v$	Volumetric heat transfer coefficient [W m <sup>-2</sup> K]
$J$	Radiosity
$K$	Permeability [m <sup>2</sup> ]
$L_a$	Thickness of a absorber [m]
$\dot{m}$	Mass flow rate [kg/s/m <sup>2</sup> ]

$P$	Pressure [Pa]
$Pr$	Prandtl number
$q_0$	Initial heat flux [ $\text{W}/\text{m}^2$ ]
$q$	Heat flux
$\hat{s}$	Unit vector in the direction of fluid flow
$T$	Temperature [K]
$u$	Velocity[m/s]
$\mathbf{V}$	Velocity vector [ $\text{m s}^{-1}$ ]

Greek symbols:

$\alpha_{sf}$	Specific surface area of the porous medium [ $\text{m}^{-1}$ ]
$\varepsilon$	Emissivity
$\phi$	Porosity
$\lambda$	Thermal conductivity [ $\text{W m}^{-1} \text{K}^{-1}$ ]
$\mu$	Dynamic viscosity [ $\text{kg m}^{-1} \text{s}^{-1}$ ]
$\beta$	Extinction coefficient [ $\text{m}^{-1}$ ]
$\tau$	Optic thickness
$\omega$	Single scattering albedo
$\Psi$	Dimensionless heat flux

subscripts

a	Average/absorber
b	Back
c	Collimated/cavity
d	Diffuse
e	Effective/environment
f	Fluid phase
r	Radiative
s	Solid phase
t	Total
v	Void
w	Wall

## 2 Model description

### 2.1 Physical model and assumptions

Figure 1 shows the schematic structure of a SiC ceramic foam air receiver or volumetric receiver is used to receive concentrated flux on its surface which is cooled directly by the pumped air. As can be seen the receiver's surface area ( $y$  direction) is much larger than its thickness ( $x$  direction). As such a one dimensional approximation in the direction of the thickness is invoked. We will also assume that the solid matrix is homogeneous and isotropic, and the variations of the thermal

properties of solid and fluid phases are neglected. Furthermore the flow is considered to be steady and fully developed.

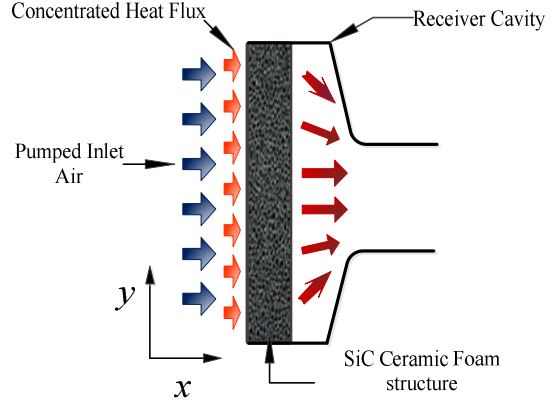


Figure 1: Schematic of the SiC ceramic foams air receiver

## 2.2 Mathematical model

### 2.2.1 Governing Equations

Continuum equation:

$$\nabla \langle \mathbf{V} \rangle = 0 \quad (1)$$

Momentum equation:

$$\frac{\rho_f}{\phi} \langle (\mathbf{V} \cdot \nabla) \mathbf{V} \rangle = \frac{\mu_f}{\phi} \nabla^2 \langle \mathbf{V} \rangle - \nabla \langle P \rangle^f - \frac{\mu_f}{K} \langle \mathbf{V} \rangle - \frac{\rho_f F \phi}{\sqrt{K}} [\langle \mathbf{V} \rangle \cdot \langle \mathbf{V} \rangle] \mathbf{J} \quad (2)$$

where the permeability  $K$ , empirical function  $F$  which depends primarily on the microstructure of the porous medium can be represented as:

$$K = \frac{\phi^3 d_p^2}{150(1-\phi)^2} \quad (3)$$

$$F = \frac{1.75}{(150\phi^{3/2})^{1/2}} \quad (4)$$

and  $\langle P \rangle^f$  is the gauge pressure and the local volume average of a quantity  $\Phi$  can be defined as  $\langle \Phi \rangle \equiv \frac{1}{V_f} \int_{V_f} \Phi dV$ ,  $\mathbf{J}$  is a unit vector oriented along the velocity vector.

Energy equations:

fluid phases:

$$(\rho c_p)_f \langle \mathbf{V} \rangle \cdot \nabla \langle T_f \rangle = \nabla \cdot (\lambda_{fe} \cdot \nabla \langle T_f \rangle) + h_{sf} a_{sf} (\langle T_s \rangle - \langle T_f \rangle) \quad (5)$$

solid phases:

$$0 = \nabla \cdot (\lambda_{se} \cdot \nabla \langle T_s \rangle - q_r) - h_{sf} a_{sf} (\langle T_s \rangle - \langle T_f \rangle) \quad (6)$$

where:

$$\lambda_{fe} = \varphi \lambda_f \quad (7)$$

$$\lambda_{se} = \varphi \lambda_s \quad (8)$$

The specific surface area of porous bed with appears in both energy equation 5 and 6 is developed based on geometrical considerations:

$$\frac{6(1-\varphi)}{d_p} \quad (9)$$

The fluid-to-solid phase heat transfer coefficient in this study was based on the empirical correlation established by (Wang P, 2015) is presented as follows:

$$h_{sf} = \left( \frac{d_p \varphi}{0.2555 Pr^{1/3} Re^{2/3} \lambda_f} + \frac{d_p}{10 \lambda_s} \right)^{-1} \quad (10)$$

The radiation parameters that is the extinction  $\beta$ , absorption  $\kappa$  and scattering coefficients  $\sigma_s$  are strongly dependent on the experimental test. (Hsu Pf, Howell JR 1992) presented a method of simultaneously inverting conductivity and extinction coefficient from the experimental data. The trend of the change of extinction coefficient had good agreement the geometric optics limit prediction (Tien CL 1988) when pore size greater than 0.6mm:

$$\beta = \frac{\Psi}{d_p} (1-\varphi) \quad (11)$$

where the value of  $\Psi$  is given as 3, other test results shows that  $\Psi$  should be change to 4.4 based on foam ceramic porous media. (Mohanraj R *et. al.* 1996) also presented the experimental test focus on the RPC material, the result shows that radiation properties is not sensitive to the temperature at the range of 1200K-1400K, detailed parameters is given as follow:

$$\kappa = (2-\varepsilon) \frac{3}{2d_p} (1-\varphi) \quad (12)$$

$$\sigma_s = \varepsilon \frac{3}{2d_p} (1-\varphi) \quad (13)$$

## 2.2.2 Radiation transfer

Under the assumption of collimated irradiation, a modified differential approximation (P-1 Model) is applied to address this problem here. We have the express for the diffuse radiative flux  $q_d$  and the incident radiation  $G_d$  as follow:

$$\nabla q_d = \kappa (4\sigma \langle T_s \rangle^4 - G_d) + \sigma_s G_c \quad (14)$$

$$q_d = -\frac{1}{3\beta} \nabla G_d \quad (15)$$

Then the differential equation for  $G_d$  is obtained as:

$$0 = \frac{1}{3\beta} \nabla G_d^2 + \kappa (4\sigma \langle T_s \rangle^4 - G_d) + \sigma_s G_c \quad (16)$$

Meanwhile  $q_c$ , the remnant collimated beam after partial extinction, by absorption and scattering, along its path in the direction which perpendicular to the horizontal boundary is given by the exact solution:

$$q_c = G_c = q_0 e^{-\beta x} \quad (17)$$

## 2.2.3 Variable porosity

The variation of the porosity in the flow direction are defined by a linear function:

$$\varphi = A_p + \left( \frac{B_p}{L_a} \right) \cdot x \quad (18)$$

where the coefficient  $A_p$  and  $B_p$  control the variation of the porosity. When the  $B_p$  is negative, it means that the porosity decreases along the flow direction, however it increase when  $B_p$  is positive.

## 2.2.4 Boundary conditions

The incident radiation flux  $q_{in}$  which is concentrated by a heliostat field can be presented by:

$$q_{in} = 1 \text{ MW/m}^2 \quad (19)$$

Radiation heat loss between the receiver's surface and environment can be represented by:

$$q_{loss} = \sigma \varepsilon \left( \langle T_{s,in} \rangle^4 - \langle T_e \rangle^4 \right) \quad (20)$$

The temperature of the inlet fluid,  $T_{f,in}$  is the same as the environment temperature  $T_e$  which is taken as

$$T_{f,in} = T_e = 300 \text{ K} \quad (21)$$

For the outlet boundary, an adiabatic boundary condition is used:

$$\left. \frac{\partial \langle T_s \rangle}{\partial x} \right|_{x=L} = 0 \quad (22)$$

$$\left. \frac{\partial \langle T_f \rangle}{\partial x} \right|_{x=L} = 0 \quad (23)$$

the diffuse radiative flux can be neglected hence the radiative boundary conditions for the

inlet and outlet are as follows:

$$\left. \frac{\partial \langle G_d \rangle}{\partial x} \right|_{x=0} = \left. \frac{\partial \langle G_d \rangle}{\partial x} \right|_{x=L} = 0 \quad (24)$$

### 3 Numerical procedure

Using a Finite Volume Method, Governing equations are discretized using a SIMPLE algorithm. The discretization scheme is based on a uniform grid set up and a cell centered scheme. Furthermore, 1st order upwind differencing method is employed to discretize the convective terms. The convergence is considered to have been reached when the relative variation of temperature between consecutive iterations is smaller than  $10^{-8}$  for all the grid points in the computational domain.

### 4 Results and discussion

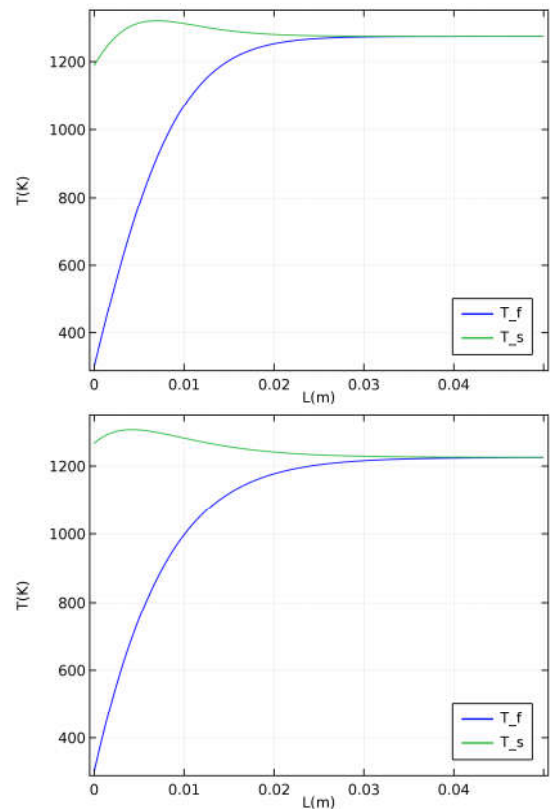
#### 4.1 Increasing porosity

Fig. 2 depicts the distribution of fluid and solid temperature  $T_f$  and  $T_s$  and heat flux  $q$  for different value of porosity  $\phi$  with constant pore diameter  $d_p=2\text{mm}$ , inlet air velocity  $U_{in}=0.5\text{m/s}$  and incident radiation  $q_0=1\text{MW}$ .

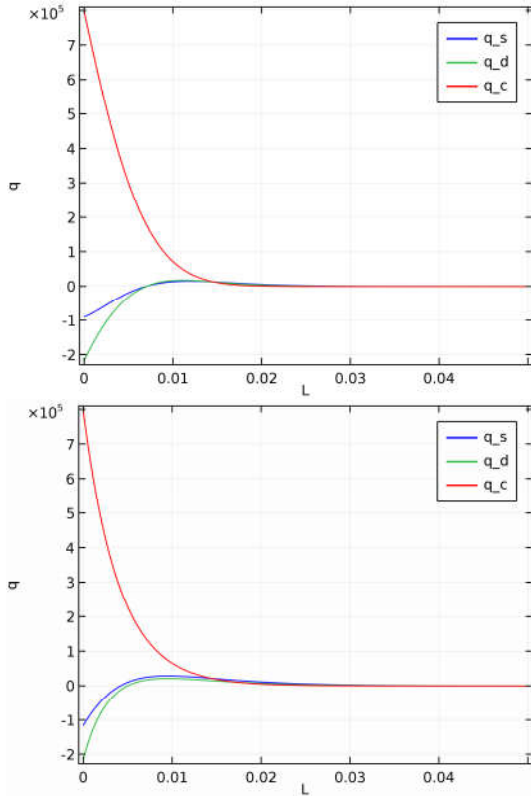
As expected in the Fig. 2a and 2b, the temperature  $T_s$  along the  $x$  direction for the solid phase is decrease in the incident direction, however, for the fluid phase temperature  $T_f$ , it increases along the  $x$  direction. It can be seen that the solid temperature  $T_s$  at the irradiated surface greatly decreases when using the variable porosity material along the  $x$  direction.  $T_s$  decreases nearly 50K when the control parameters  $A_p=0.9$  and  $B_p=-0.3$ . The outlet air temperature at the back wall of the absorber increases when using the variable porosity material, this is because that the lower surface temperature decreases the radiative loss, consequently the efficiency increased accordingly.

Fig. 3a, and 3b present that both of the variation value of the extinct collimated radiative flux  $q_c$ , diffuse radiative flux  $q_d$  and conductive heat flux  $q_s$  along the  $x$  direction. It can be seen that the incident radiative energy here we assume as the gradient of the collimated

irradiation attenuation decreases sharply along the incident direction of the porous media. This part can be taken as the volumetric energy source distributed in the porous media. Hence, with its decrease the heat flux absorbed by the porous media decreases. However the diffuse radiative  $q_d$  increases first and then decrease slightly, this is because the diffuse radiative flux  $q_d$  dependent on not only the solid temperature  $T_s$  but also the distribution of the incident irradiation  $q_c$ . For the conductive heat flux  $q_s$  in the solid phase (see Fig. 3a, 3b), the effect of the porosity on its distribution has a reverse rule compared to that on the diffuse radiative flux. This shows the limiting interactions between thermal radiation and conduction. When comparing the Fig 3a, 3b we can also found that the conductive heat flux  $q_s$  decreases slightly at the irradiated surface.

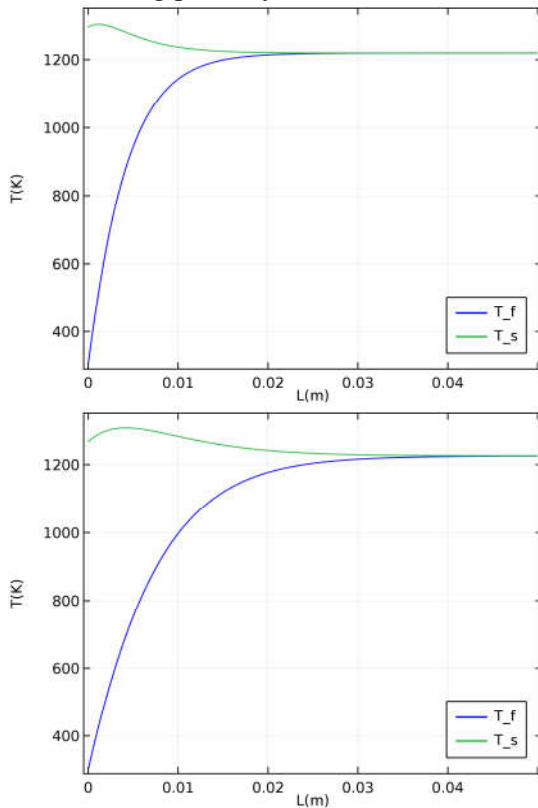


(a) Variable porosity (b) Constant porosity  
Fig. 2: Effect of the porosity on the temperature and heat flux in the  $x$  direction ( $A_p=0.9$ ,  $B_p=-0.3$ )



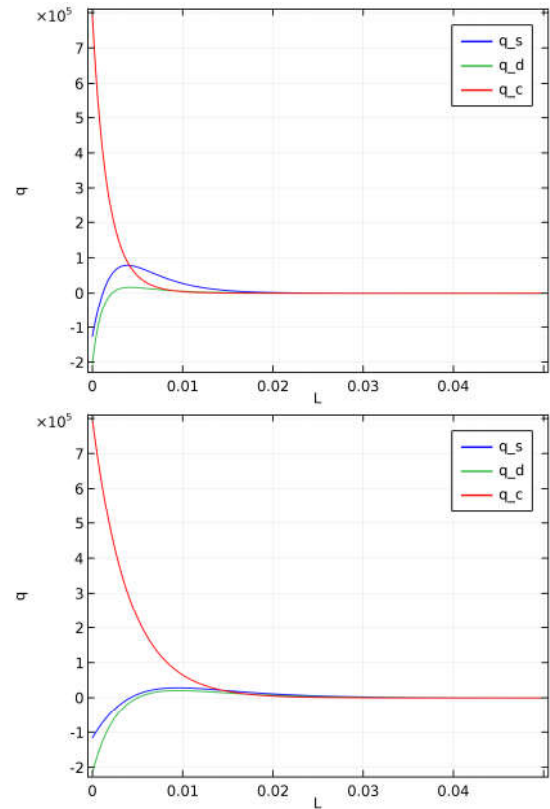
(a) Variable porosity (b) Constant porosity  
 Fig. 3: Effect of the porosity on the heat flux in the  $X$  direction ( $A_p=0.9, B_p=-0.3$ )

#### 4.2 Decreasing porosity



(a) Variable porosity (b) Constant porosity

Fig. 4: Effect of the porosity on the temperature and heat flux in the  $X$  direction ( $A_p=0.9, B_p=-0.3$ )



(a) Variable porosity (b) Constant porosity  
 Fig. 5: Effect of the porosity on the heat flux in the  $X$  direction ( $A_p=0.9, B_p=-0.3$ )

Fig. 4 and 5 depicts the distribution of fluid and solid temperature  $T_f$  and  $T_s$  and heat flux  $q$  for different arrangement of porosity  $\phi$  with constant pore diameter  $d_p=2\text{mm}$ , inlet air velocity  $U_{in}=0.5\text{m/s}$  and incident radiation  $q_0=1\text{MW}$ .

For this case, in the Fig. 4a and 4b, It can be seen that the solid temperature  $T_s$  at the irradiated surface greatly increases when using the variable porosity material along the  $x$  direction.  $T_s$  increases nearly 20K when the control parameters  $A_p=0.6$  and  $B_p=0.3$ . The outlet air temperature at the back wall of the absorber decreases when using the variable porosity material, this is because that the lower surface temperature increases the radiative loss, consequently the efficiency decreased accordingly. When comparing the Fig 5a and 5b we can also found that the conductive heat flux  $q_s$  decreases more slightly at the irradiated

surface for the variable porosity, which is due to the high temperature gradient of the solid phase with variable porosity effect.

## CONCLUSIONS

Convective and radiative transport in a air receiver using porous media in the presence of collimated irradiation and local thermal non-equilibrium is analyzed in this work. A modified P-1 approximation with collimated irradiation was introduced to incorporate the radiative transfer. We analyzed the distribution of the temperature of the fluid and solid phase, also the heat flux in the incident direction was presented. Based on our analysis, it can be seen that the incident radiative energy i.e. the collimated irradiation attenuation sharply along the incident direction of the porous media. The temperature  $T_s$  along the  $x$  direction is decrease for the solid phase but increases for the fluid phase temperature  $T_f$  along the  $x$  direction. The diffuse radiative  $q_d$  increases first and then decrease, this is because the diffuse radiative flux not only dependent on the solid temperature but also the distribution of the incident irradiation i.e. the extinction part of collimated irradiation  $q_c$ . Lower solid temperature can be achieved by using a variable porosity. The porosity and pore diameter has a non-monotonic effect on the thermal efficiency of the receiver, optimization can be achieved by further parameters analysis.

## ACKNOWLEDGEMENT

The support of the National Natural Science Foundation of China (No.51209073), Natural Science Foundation of Jiangsu Province (No.BK20150816). The authors also gratefully acknowledge the financial support from the National High-tech R&D Program of China (863 Program) of Chinese Science and Technology Department under Project Numbers No. 2007AA05Z445.

## REFERENCES

Aacutevila AL 2011. "Volumetric receivers in Solar Thermal Power Plants with Central Receiver System technology: A review," *Solar Energy*, vol. 85, pp. 891-910.

Alazmi B, Vafai K 2000. "Analysis of Variants Within the Porous Media Transport Models," *Journal of Heat Transfer*, vol. 122, pp. 303-326.

Flamant G, Olalde G 1983. "High temperature solar gas heating comparison between packed and fluidized bed receivers—I," *Solar Energy*, vol. 31, pp. 463-471.

Hsu Pf, Howell JR 1992. "Measurement of thermal conductivity and optical properties of porous partially stabilized zirconia," *Experimental Heat Transfer*, vol. 5, pp. 293-313.

Mohanraj R *et. al.* 1996. "Measurements of radiative properties of cellular ceramics at high temperatures," *Journal of Thermophysics and Heat Transfer*, vol. 10, pp. 33-38

Singh BP, Kaviany M 1991. "Independent theory versus direct simulation of radiation heat transfer in packed beds," *International Journal of Heat and Mass Transfer*, vol. 34, pp. 2869-2882.

Tien CL 1988. "Thermal-Radiation in Packed and Fluidized-Beds," *Journal of Heat Transfer ASME*, vol. 110, pp. 1230-1242.

Wang P, Vafai K, and Liu DY 2014. "Analysis of Radiative Effect under Local Thermal Non-Equilibrium Conditions in Porous Media-Application to a Solar Air Receiver," *Numerical Heat Transfer Part a-Applications*, vol. 65, pp. 931-948.

Wang P, Vafai K, and Liu DY 2015 "Analysis of collimated irradiation under local thermal non-equilibrium condition in a packed bed," *International Journal of Heat and Mass Transfer*, vol. 80, pp. 789-801.

Yang K, Vafai K 2010. "Analysis of temperature gradient bifurcation in porous media - An exact solution," *International Journal of Heat and Mass Transfer*, vol. 53, pp. 4316-4322